The Design of High Dynamic Range Continuous-Time Integratable Bandpass Filters

Gert Groenewold

Abstract—**A method to design integratable continuous-time analog high-Q bandpass filters with a *prescribed* dynamic range is developed. The theory accompanying this method shows what the fundamental restrictions for the dynamic range are. The theory is meant to determine beforehand if the dynamic range one wants is realizable. The possibilities of using dynamic range optimal filter networks are discussed. A design example is included.**

I. Introduction

SINCE integrated circuit technology offers possibilities to realize integrated continuous-time analog filters, international interest in this subject is aroused. In the last ten years many articles about the realization of this kind of filters have been published; [1]–[6] are just a few examples.

There is, however, no general design theory available. In all cases we have met in literature, design is started by choosing a filter network, realizing this network actively, and evaluating the performance afterwards. Usually the only link between the expected performance and the network established is the remark that the network was known to behave well in a passive realization. Of course this is a valid way to design filters, but when it comes to designing high-performance filters, this method has limited use. In this article we concentrate on dynamic range as performance parameter and want to make an attempt at the establishing of a theory that makes it possible to design a high-Q (that is, narrow-band) bandpass filter satisfying a dynamic range demand that is stated *beforehand*. Using this theory we also are able to say what the *optimal* dynamic range belonging to a certain transfer function under certain technological constraints is so that one can say something of the quality of a particular filter network. This makes a scientifically responsible choice for a filter network possible. Optimal networks can be found, but this is not the most important thing, for optimal networks are usually too difficult to realize, and more conventional structures sometimes come close enough to the optimum.

The dynamic range of integratable continuous-time analog filters is a serious problem. The reason for this is that because this kind of filter must be made tunable [4], nonlinear elements are introduced in their circuits. As all known realizations of these filters (also, for instance, the gyrator type and Sallen and Key type filters) can be viewed as a network of n integrators—where n is the order of the filter—the dynamic range of a filter, given the filter transfer function, is dependent on

- the dynamic range of the network elements, that is, of the integrators used, and
- the filter network architecture.

Many realizations of integratable tunable integrators have been proposed, having different dynamic range properties. The realization of the integrators will not be the subject of this paper. Instead, we will see how the dynamic range of a filter is dependent on the network used; the properties of the integrators will be assumed to be known.

Special attention must be devoted to the subclass of bandpass filters because most of the effects of the nonidealities (such as parasitic poles, inaccuracies, limited dynamic range) of the filter components on the filter performance are proportional to Q [3]. The dynamic range, especially, of this class of filters is a problem. Usually, the noise output of high-Q filters appears to be directly proportional to Q [3], a fact that has led many authors to the belief that the dynamic range of a high-Q filter is inversely proportional to its quality factor [3], [5].

This is an important result that reflects a fundamental restriction on the possibilities of realizing high-Q bandpass filters. However, it is not clear that this is really a fundamental property of this class of filters. For any given transfer function, an infinite amount of possible realizations exists, and who knows if all these realizations share this property? Indeed, a biquad has been reported that features an output noise level, which is independent of its quality factor [7]. From this the conclusion was drawn that in principle it is possible to construct a biquad with a

Manuscript received March 23, 1990; revised July 9, 1990. This work was supported by the Dutch Innovative Research Projects Fund. This paper was recommended by Associate Editor T. T. Vu.

The author is with the Department of Electrical Engineering, Delft University of Technology, Delft, The Netherlands.

IEEE Log Number 9100872.

0098-4094/91/0800-0838$01.00 ©1991 IEEE

More — on the outside.

quality factor independent dynamic range, a conclusion that in this paper will be proven wrong.

To formulate the theories involved, we will first point out how the relatively well-known concept of the state-space representation for dynamical systems can be used as a convenient tool for the description and the optimization of the architecture of a filter. After that, we will state a definition of dynamic range. Using this, we tackle the problem of optimizing high-Q second-order filter structures (biquads). A general optimization procedure that has been developed for digital filters [10] will be adapted for the case of analog continuous-time filters. We will build upon this theory, with use of our results for biquads, an optimization theory and method for bandpass filters. This theory will give valuable insights into the fundamental limits that exist for the realizability of high-Q bandpass filters.

Using this theory we develop a design theory for high dynamic range bandpass filters. In the end we will discuss the complete design of a practical filter in the light of the newly developed theories.

In order to save space, most of the lengthy mathematical proofs are omitted. These are included in an internal report [8].

II. State-Space Representation

In this paper we will represent the internal structure of filters by the *state-space representation*. In this representation an nth-order filter comprises n integrators. The output signals x_i $(1 \leqslant i \leqslant n)$ of these integrators are taken together in the $(n \times 1)$ *state vector* $\boldsymbol{X}$. The input signal of the filter is denoted by E_i and its output signal by E_o. The state equations that describe the filter are

$$s\boldsymbol{X} = \boldsymbol{A}\boldsymbol{X} + \boldsymbol{B}E_i \tag{1}$$

$$E_o = \boldsymbol{C}\boldsymbol{X} + \boldsymbol{D}E_i. \tag{2}$$

$\boldsymbol{A}$, $\boldsymbol{B}$, and $\boldsymbol{C}$ are matrices; $\boldsymbol{D}$ is a scalar. The transfer function of the filter is then

$$H(s) \overset{\text{def}}{=} \frac{E_o(s)}{E_i(s)} = \boldsymbol{C}(s\boldsymbol{I} - \boldsymbol{A})^{-1}\boldsymbol{B} + \boldsymbol{D}. \tag{3}$$

$\boldsymbol{I}$ denotes the proper identity matrix.

Using this model, the internal transfer functions f_i and g_i can be computed. The functions f_i are the transfer functions from the input of the filter to the output of integrator i, that is, x_i. The functions g_i are the transfer functions from the input of integrator i, that is, sx_i, to the output of the filter. The functions f_i are important for the calculation of the maximum input signal level of the filter, while the functions g_i are used to calculate the total noise output of the filter. The noise level and maximum signal level are needed to calculate the dynamic range of the filter.

The functions f_i and g_i are put together into the vectors $\boldsymbol{F}$ and $\boldsymbol{G}$ as follows:

$$\boldsymbol{F} = \begin{pmatrix} f_1 \\ f_2 \\ \vdots \\ f_n \end{pmatrix} \tag{4}$$

$$\boldsymbol{G} = (g_1, g_2, \cdots, g_n). \tag{5}$$

$\boldsymbol{F}$ and $\boldsymbol{G}$ can be easily computed:

$$\boldsymbol{F} = (s\boldsymbol{I} - \boldsymbol{A})^{-1}\boldsymbol{B} \tag{6}$$

$$\boldsymbol{G} = \boldsymbol{C}(s\boldsymbol{I} - \boldsymbol{A})^{-1}. \tag{7}$$

Of considerable importance for the optimization of the dynamic range are the so-called observability and controllability gramian matrices $\boldsymbol{W}$ and $\boldsymbol{K}$ [10], defined as follows:

$$\boldsymbol{W} = \frac{1}{2\pi}\int_{-\infty}^{\infty} \boldsymbol{G}^*\boldsymbol{G}\,d\omega \tag{8}$$

$$\boldsymbol{K} = \frac{1}{2\pi}\int_{-\infty}^{\infty} \boldsymbol{F}\boldsymbol{F}^*\,d\omega. \tag{9}$$

The asterisk (*) denotes the adjoint operator, so if $\boldsymbol{M}$ is an arbitrary matrix, $\boldsymbol{M}^*$ is the transpose of the matrix of complex conjugates of the elements of $\boldsymbol{M}$: $\boldsymbol{M}^* = \overline{\boldsymbol{M}}^T$. It is not difficult to prove that $\boldsymbol{K}$ and $\boldsymbol{W}$ are positive definite.

One can also prove that $\boldsymbol{W}$ and $\boldsymbol{K}$ satisfy the following equations.

$$\boldsymbol{A}^T\boldsymbol{W} + \boldsymbol{W}\boldsymbol{A} = -\boldsymbol{C}^T\boldsymbol{C} \tag{10}$$

$$\boldsymbol{A}\boldsymbol{K} + \boldsymbol{K}\boldsymbol{A}^T = -\boldsymbol{B}\boldsymbol{B}^T. \tag{11}$$

These equations have unique solutions if and only if the filter has not more than one pole on the imaginary axis.

III. Dynamic Range

The dynamic range of an arbitrary signal processing system is the ratio of the maximal and minimal signal levels that can be processed in that system. The minimum level is determined by the noise performance of the system, the maximum level by distortion.

Usually, as maximal signal level the level where 1% or 0.1% total harmonic distortions occurs, or where the distortion level equals the noise level, is used. This maximal signal level (at the input or output of the system, however defined) will be denoted by $U_{\max}$. If the noise level at the same point is denoted by U^2_{noise} (the mean squared noise voltage) the dynamic range (denoted by DR) is

$$DR = \frac{U^2_{\max}}{U^2_{\text{noise}}}. \tag{12}$$

To determine the dynamic range of filters we will now discuss the noise generation of filters, using the state-space representation.

More — on the outside.

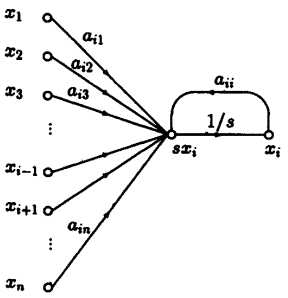

Fig. 1. A part of a filter: One integrator with its connections to its surroundings.

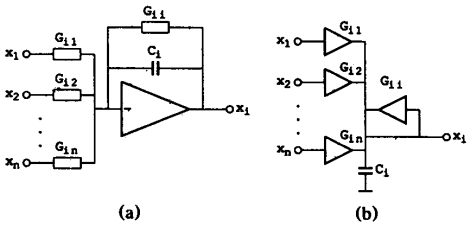

Fig. 2. Two examples of a practical realization of the structure depicted in Fig. 1.

IV. Noise

Fig. 1 shows a part of an nth-order filter. This part consists of one integrator, the input of which is connected to the outputs of the n other integrators, including its own output. From now on, the branch which is denoted by $1/s$ in this figure will be called an *intrinsic* integrator. The complete structure shown in Fig. 1 (the intrinsic integrator together with all the branches that are connected to its input) can be seen as a multiple input integrator and will be called an *extrinsic* integrator. The number of the integrator is i, which means that the output signal of this integrator is x_i. The a_{ij} in this figure are entries of the matrix A. The transfer function that this part of the filter network realizes from x_j to x_i is a_{ij}/s, and can be realized in various ways. Fig. 2 shows two examples. In Fig. 2(a) the time constants are realized with conductances and capacitors, and in Fig. 2(b) with transconductances and capacitors.

Here, $|a_{ij}| = G_{ij}/C_i$. C_i is the capacitance value of the integrating capacitor. The G_{ij} are the values of the input (trans)conductances. The noise voltage spectrum at input j of extrinsic integrator i is

$$S_{\mathrm{ni},ij}(\omega) = \xi\frac{2kT}{G_{ij}} = \xi\frac{2kT}{|a_{ij}|C_i}. \tag{13}$$

The factor ξ is the noise factor of the (trans)conductances G_{ij}.

The output referred noise voltage spectrum of integrator i is thus

$$S_{\mathrm{no},i}(\omega) = \sum_{j=1}^{n}\left(\frac{a_{ij}}{\omega}\right)^2 S_{\mathrm{ni},ij}(\omega) = \frac{2kT\xi}{C_i\omega^2}\sum_{j=1}^{n}|a_{ij}|. \tag{14}$$

This spectrum can be transformed to the spectrum of a noise voltage source that adds to the *input* of the *intrinsic* integrator. In that case the spectrum is

$$S_{\mathrm{n},i}(\omega) = \frac{2kT\xi}{C_i}\sum_{j=1}^{n}|a_{ij}|. \tag{15}$$

The noise production due to the branch b_i (b_i is an element of B) can be added to this in the same way. Thus we find for the total input referred noise spectrum of *intrinsic* integrator i:

$$S_{\mathrm{n},i}(\omega) = \frac{2kT\xi}{C_i}\left(|b_i| + \sum_{j=1}^{n}|a_{ij}|\right). \tag{16}$$

The influence of the b_i can always be made negligible. This is done by scaling these entries down until they are not dominant in the noise production anymore. By (3), scaling the b_i down by a factor means that H is scaled down by the same factor. This can be compensated for by additional amplification at the input or output of the filter (which can always be done with negligible additional noise production [9]) or by scaling the entries c_i of C up. Therefore, for optimization purposes, we will use (15) as the expression for the noise spectra.

We will not consider $1/f$-noise here. This is not necessary in the case of high-Q bandpass filters because then the frequencies of interest usually are so high that this kind of noise has no influence. In the cases that $1/f$-noise is important, the bandwidth of the filters will be so narrow that this noise can be considered white and can be incorporated in the noise factor ξ.

The expressions for the internal noise sources are used to find an expression for the dynamic range. Before we do so we discuss the notion of scaling a filter in order to improve its dynamic range.

V. Scaling and Norms

One way to improve the dynamic range of a filter is *scaling*. The purpose of scaling is to make the output signal levels of all the integrators in the filter equal, so that there is not a single integrator in the filter that limits the maximal input signal level. It is not trivial that this approach yields a maximum dynamic range, because in the process of scaling the filter the noise spectra are altered, a fact that must be accounted for. It can, however, be proved that an optimal filter is scaled.

The information carrying the input signal of the filter is represented by a white noise signal. In that case the filter is scaled if the squared ℓ_2-norms of the internal transfers f_i, defined as

$$|f_i|_2^2 = \frac{1}{2\pi}\int_{-\infty}^{\infty}|f_i(j\omega)|^2\,d\omega \tag{17}$$

are equal.

The squares of the ℓ_2-norms of the g_i are the noise integrals, so the total noise output of the filter can be expressed as

$$\overline{U_{n,o}^2} = \sum_{i=1}^{n} S_{n,i} \frac{1}{2\pi} \int_{-\infty}^{\infty} |g_i(j\omega)|^2 \, d\omega = \sum_{i=1}^{n} S_{n,i} |g_i|_2^2. \quad (18)$$

Here, $\overline{U_{n,o}^2}$ is the mean square value of the output noise voltage of the filter and $S_{n,i}$ denotes the noise power spectrum at the input of integrator i. To emphasize the fact that this spectrum is assumed to be a constant function (the spectrum is white), it is denoted by the constant $S_{n,i}$.

We note here that the squares of the ℓ_2-norms of the f_i and the g_i are the diagonal elements of the gramians $\boldsymbol{W}$ and $\boldsymbol{K}$:

$$w_{ii} = |g_i|_2^2 \qquad k_{ii} = |f_i|_2^2 \quad (19)$$

as can easily be seen from (8) and (9). With this result the total output noise level (18) can be written as

$$\overline{U_{n,o}^2} = \sum_{i=1}^{n} S_{n,i} w_{ii}. \quad (20)$$

Now suppose that we want to scale the filter, so that all the squared ℓ_2-norms of the f_i equal κ. Then the diagonal entries of $\boldsymbol{W}$, expressed in the gramians of the filter before scaling are [10]

$$\hat{w}_{ii} = \frac{k_{ii} w_{ii}}{\kappa}. \quad (21)$$

$\hat{\boldsymbol{W}}$ is the observability gramian of the scaled filter.

Using (20) and (21), an expression for the total noise output of the scaled filter can be found:

$$\overline{\hat{U}_{n,o}^2} = \sum_{i=1}^{n} \hat{S}_{n,i} \frac{k_{ii} w_{ii}}{\kappa}. \quad (22)$$

Here, $\hat{S}_{n,i}$ is the spectrum of the input referred noise voltage source of intrinsic integrator i in the *scaled* filter. The matrices $\boldsymbol{K}$ and $\boldsymbol{W}$ in this equation refer to the filter *before* scaling.

Scaling is a method to improve the dynamic range of a filter without altering the filter network architecture. Before methods to optimize filter architectures are discussed, the dynamic range as defined in Section III is evaluated using results derived thus far.

VI. Dynamic Range of Filters

With the results of the previous sections we can find an expression for the dynamic range of an arbitrary filter. The dynamic range of a filter is defined as the ratio of the maximum signal level at the input or output of a filter and the noise level at the same point. We will use the output of the filter for our calculations.

Suppose that to the input of the filter a white noise signal (representing an information carrying signal) is applied. The spectrum of this signal is $S_{in}(\omega)$. With this kind of input signal the relevant measure for the signal level is the ℓ_2-norm. The mean square of the resulting output signal of integrator i is

$$\overline{U_{s,i}^2} = S_{in} \cdot k_{ii}. \quad (23)$$

(The subscript s stands for signal; n stands for noise.) Suppose that the maximum allowed mean square of the output signals of the integrators is U_{max}^2. In that case the maximum allowed value of S_{in} is:

$$S_{max,in} = \frac{U_{max}^2}{\max_i k_{ii}}. \quad (24)$$

The mean square of the corresponding output signal will be:

$$\overline{U_{max,out}^2} = S_{max,in} \frac{1}{2\pi} \int_{-\infty}^{\infty} |H(j\omega)|^2 \, d\omega. \quad (25)$$

The total noise output of the filter is expressed by (20). This yields the dynamic range:

$$DR = \frac{\overline{U_{max,out}^2}}{\overline{U_{n,o}^2}} = \frac{U_{max}^2 \frac{1}{2\pi} \int_{-\infty}^{\infty} |H(j\omega)|^2 \, d\omega}{\sum_{i=1}^{n} S_{n,i} w_{ii} \max_j k_{jj}}. \quad (26)$$

If we scale the filter such that we make all k_{ii} equal κ, $\max_j k_{jj}$ equals κ. The output noise level is then given by (22), so the dynamic range is then

$$DR = \frac{\overline{U_{max,out}^2}}{\overline{\hat{U}_{n,o}^2}} = \frac{U_{max}^2 \frac{1}{2\pi} \int_{-\infty}^{\infty} |H(j\omega)|^2 \, d\omega}{\sum_{i=1}^{n} \hat{S}_{n,i} k_{ii} w_{ii}}. \quad (27)$$

This is the dynamic range of the *scaled* filter in terms of the $\boldsymbol{K}$ and $\boldsymbol{W}$ of the filter *before* scaling. Note that the dynamic range does not depend on κ.

In practical cases we must integrate H to determine the dynamic range from this equation. It is easy to prove from (3), (6), (7), (8), and (9) that

$$\frac{1}{2\pi} \int_{-\infty}^{\infty} |H(j\omega)|^2 \, d\omega = \boldsymbol{CKC}^T = \boldsymbol{B}^T \boldsymbol{WB}. \quad (28)$$

This can offer a handy way to perform this integration.

We proceed on how to optimize expressions (26) and (27).

VII. Dynamic Range of Biquads

In this section the dynamic range of high-Q biquads is evaluated and optimized. In subsequent sections the results derived here for high-Q biquads are used to evaluate and optimize the dynamic range of high-Q bandpass filters.

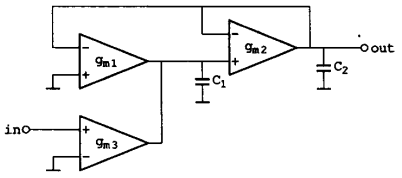

Fig. 3. An example of a biquad.

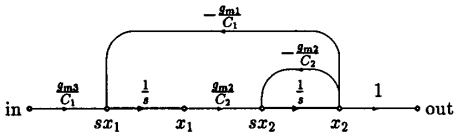

Fig. 4. The signal flow graph of the filter of Fig. 3.

7.1. Example

An example of a biquad is shown in Fig. 3. This biquad has been taken from literature [7], where it was claimed that its output noise voltage was independent of its quality factor, from which the conclusion was drawn that this biquad featured a quality factor independent dynamic range. This statement is interesting enough to induce us to evaluate the dynamic range of this biquad.

The signal flow graph of this biquad is shown in Fig. 4. The state matrices are

$$\boldsymbol{A}=\begin{pmatrix} 0 & -\frac{g_{m1}}{C_1} \\ \frac{g_{m2}}{C_2} & -\frac{g_{m2}}{C_2} \end{pmatrix}, \qquad \boldsymbol{B}=\begin{pmatrix} \frac{g_{m3}}{C_1} \\ 0 \end{pmatrix},$$

$$\boldsymbol{C}=(0 \quad 1), \qquad \boldsymbol{D}=0. \tag{29}$$

From this, by (3):

$$H(s)=\frac{\frac{g_{m2}g_{m3}}{C_1C_2}}{s^2+\frac{g_{m2}}{C_2}s+\frac{g_{m1}g_{m2}}{C_1C_2}}=\frac{N(s)}{D(s)} \tag{30}$$

in which

$$D(s)\overset{\text{def}}{=}s^2+\frac{\omega_0}{Q}s+\omega_0^2 \tag{31}$$

so

$$\omega_0=\sqrt{\frac{g_{m1}g_{m2}}{C_1C_2}} \tag{32}$$

$$Q=\sqrt{\frac{C_2g_{m1}}{C_1g_{m2}}}. \tag{33}$$

By substituting (29) into (16) we can directly determine the input referred noise spectra of the intrinsic integrators:

$$S_{n,1}=\frac{2kT\xi}{C_1}\left(\frac{g_{m3}}{C_1}+\frac{g_{m1}}{C_1}\right)=\frac{2kT\xi(g_{m1}+g_{m3})}{C_1^2} \tag{34}$$

$$S_{n,2}=\frac{2kT\xi}{C_2}\left(\frac{g_{m2}}{C_2}\right)=\frac{2kT\xi g_{m2}}{C_2^2}. \tag{35}$$

In the case of $S_{n,2}$ the two branches a_{21} and a_{22} only give rise to one noise source because these two branches are realized with only one transadmittance stage.

The matrix $\boldsymbol{W}$ can be determined by solving (10), which results in

$$\boldsymbol{W}=\begin{pmatrix} \frac{C_1}{2g_{m1}} & 0 \\ 0 & \frac{C_2}{2g_{m2}} \end{pmatrix}. \tag{36}$$

The total noise output of the filter is determined with (18) and (19) as

$$\overline{U_{n,o}^2}=S_{n,1}w_{11}+S_{n,2}w_{22}=kT\xi\left(\frac{1}{C_2}+\frac{1}{C_1}\left(1+\frac{g_{m3}}{g_{m1}}\right)\right). \tag{37}$$

Now g_{m3} can be chosen freely because it does not influence ω_0 or Q. We thus may choose $g_{m3} \ll g_{m1}$, and the expression for the output noise voltage is

$$\overline{U_{n,o}^2}=kT\xi\left(\frac{1}{C_1}+\frac{1}{C_2}\right). \tag{38}$$

We see that the output noise level is indeed independent of Q, and depends only on the noise properties of the integrators.

To complement the calculation of the dynamic range of the biquad we determine its maximal output signal level. Therefore, we determine $\boldsymbol{K}$ by solving (11).

$$\boldsymbol{K}=\frac{g_{m3}^2}{2g_{m1}C_1}\begin{pmatrix} 1+Q^2 & 1 \\ 1 & 1 \end{pmatrix}. \tag{39}$$

Then by (24), (25), and (28), we have

$$U_{\max,\text{out}}^2=\frac{U_{\max}^2}{\max(1+Q^2,1)}\simeq\frac{U_{\max}^2}{Q^2}. \tag{40}$$

Now the dynamic range of this biquad can be determined:

$$DR=\frac{U_{\max,\text{out}}^2}{\overline{U_{n,o}^2}}=\frac{U_{\max}^2}{kT\xi Q^2\left(\frac{1}{C_1}+\frac{1}{C_2}\right)}. \tag{41}$$

This can be optimized by dividing the total capacitance C available optimally between C_1 and C_2. The optimum is found if $C_1=C_2=C/2$. This gives us the optimized dynamic range for this biquad:

$$DR_{\text{opt}}=\frac{U_{\max}^2C}{4kT\xi}\frac{1}{Q^2}. \tag{42}$$

The first conclusion is clear. Even though the noise output of the biquad is independent of its quality factor, the dynamic range definitely is not. In the next section we will see that the dynamic range of an optimal biquad is inversely proportional to its quality factor, while the dynamic range of this biquad is even inversely proportional to the *square* of its quality factor, so this biquad is a profoundly bad one.

We might turn to the question why this biquad is so bad. Basically this is a consequence of the fact that the k_{ii} (see (39)) differ so much (a factor Q^2) from each other, meaning that the filter is far from being scaled.

From this example it should be clear that careful reasoning is necessary. It is a very commonly made mistake that only the noise output of filters is regarded and that distortion and inherent maximum signal levels are discarded or, if they are regarded, it is assumed that the maximal output signal level of the filter equals the maximal output signal level of the integrators. It should by now be clear that that is not necessarily true. To be concrete at this point we refer to (40).

7.2. General

In the previous section we evaluated the dynamic range of a specific biquad. In this section we will optimize high-Q biquads in a general way, thus arriving at fundamental dynamic range limits.

A biquad is a second-order filter; it therefore has a second-order set of state matrices:

$$\boldsymbol{A}=\begin{pmatrix} a_{11} & a_{12} \\ a_{21} & a_{22} \end{pmatrix}, \qquad \boldsymbol{B}=\begin{pmatrix} b_1 \\ b_2 \end{pmatrix},$$

$$\boldsymbol{C}=\begin{pmatrix} c_1 & c_2 \end{pmatrix}, \qquad \boldsymbol{D}=(d). \tag{43}$$

As we assume that $|H|$ approaches zero for large $|s|$, we have $d=0$.

Using (43) with $d=0$ and (3), H can be calculated, resulting in

$$H(s)=\frac{(s-a_{22})b_1c_1+a_{12}b_2c_1+a_{21}b_1c_2+(s-a_{11})b_2c_2}{D(s)} \tag{44}$$

$$D(s)=s^2-s(a_{11}+a_{22})+a_{11}a_{22}-a_{12}a_{21}. \tag{45}$$

So from (31),

$$\omega_0=\sqrt{a_{11}a_{22}-a_{12}a_{21}} \tag{46}$$

$$\frac{\omega_0}{Q}=-(a_{11}+a_{22}). \tag{47}$$

If $Q\gg 1$ we thus see that $|a_{11}+a_{22}|\ll\omega_0$. For a stable biquad $Q>0$, and so $a_{11}+a_{22}<0$. If the components of the biquad (i.e., the damped integrators) are also stable—which will be the case in all practical situations—$a_{11}<0$ and $a_{22}<0$, so that for high-Q filters,

$$|a_{11}|\ll\omega_0 \tag{48}$$

$$|a_{22}|\ll\omega_0. \tag{49}$$

Therefore, we may assume:

$$\omega_0=\sqrt{-a_{12}a_{21}} \tag{50}$$

$$Q=\frac{\sqrt{-a_{12}a_{21}}}{-(a_{11}+a_{22})}. \tag{51}$$

To determine and optimize the dynamic range we first determine $\boldsymbol{K}$ by substituting (43) into (11) and solving for $\boldsymbol{K}$. This yields

$$\begin{pmatrix} k_{11} \\ k_{12} \\ k_{22} \end{pmatrix}=\frac{Q}{2\omega_0^3}\begin{pmatrix} \omega_0^2+a_{22}^2 & -2a_{12}a_{22} & a_{12}^2 \\ -a_{21}a_{22} & 2a_{11}a_{22} & -a_{11}a_{12} \\ a_{21}^2 & -2a_{11}a_{21} & \omega_0^2+a_{11}^2 \end{pmatrix}\begin{pmatrix} b_1^2 \\ b_1b_2 \\ b_2^2 \end{pmatrix} \tag{52}$$

and

$$k_{12}=k_{21}. \tag{53}$$

With (48) and (49) we derive from this:

$$k_{11}\simeq\frac{Q}{2\omega_0^3}(\omega_0^2b_1^2+a_{12}^2b_2^2) \tag{54}$$

and

$$k_{22}\simeq\frac{Q}{2\omega_0^3}(a_{21}^2b_1^2+\omega_0^2b_2^2). \tag{55}$$

As told, the dynamic range is optimal if the filter is scaled, so k_{11} and k_{22} should be equal. With (50) as constraint, we see that this implies that

$$|a_{12}|=|a_{21}|=\omega_0 \tag{56}$$

$$a_{12}=-a_{21}. \tag{57}$$

If these constraints are met, the nondiagonal entries of $\boldsymbol{K}$ are small compared to the diagonal entries. Therefore, for our purposes we may approximate $\boldsymbol{K}$ as

$$\boldsymbol{K}\simeq\frac{Q(b_1^2+b_2^2)}{2\omega_0}\boldsymbol{I}_2 \tag{58}$$

where $\boldsymbol{I}_2$ is the (2×2) identity matrix.

In the same way we derive for $\boldsymbol{W}$:

$$\boldsymbol{W}\simeq\frac{Q(c_1^2+c_2^2)}{2\omega_0}\boldsymbol{I}_2. \tag{59}$$

To calculate the total noise output of the filter we turn to (15), which gives an expression for the input referred noise spectrum of the intrinsic integrators. By (48), (49), and (56), the noise production corresponding to a_{11} and a_{22} is negligible compared to the influence of a_{12} and a_{21}. This gives us the total input referred noise spectrum of the intrinsic integrators for this particular high-Q biquad case:

$$S_{n,i}(\omega)=\frac{2kT\xi\omega_0}{C_i}. \tag{60}$$

With (28) we see:

$$\frac{1}{2\pi}\int_{-\infty}^{\infty}|H(j\omega)|^2\,d\omega=\frac{Q(b_1^2+b_2^2)(c_1^2+c_2^2)}{2\omega_0}. \quad (61)$$

Substituting data from (58), (59), (60), and (61) in (26) yields an expression for the dynamic range:

$$DR=\frac{U_{\max}^2}{kT\xi Q\left(\frac{1}{C_1}+\frac{1}{C_2}\right)}. \quad (62)$$

This value is not dependent on b_i and c_i, which simplifies our problem. The degree of freedom still left to be used for optimization is the division of the total capacitance C available. It is easy to see that an optimum is found for $C_1=C_2=C/2$, and the optimal dynamic range of the biquad is

$$DR_{\text{opt}}=\frac{U_{\max}^2 C}{4kT\xi}\frac{1}{Q}. \quad (63)$$

This expression gives the optimal dynamic range of a high-Q biquad as a product of two terms. The first term is an expression for the dynamic range of one integrator; the second term is the reciprocal value of the quality factor of the biquad. This expresses the fundamental quality factor dependence of the dynamic range of high-Q filters which has now been shown for the biquad case.

Summarizing this section, we may state that a high-Q biquad is dynamic range optimal if the following two conditions are met:

$$C_1=C_2=\frac{C}{2} \quad (64)$$

$$|a_{12}|=|a_{21}|=\omega_0. \quad (65)$$

Also, the noise production due to b_1 and b_2 must be made negligible. The optimal dynamic range is then given by (63).

We will use the optimization results we derived for high-Q biquads for the more general field of optimization of high-Q bandpass filters. For this end we first show how bandpass filters can be designed using frequency transformations.

VIII. Frequency Transformation

8.1. Biquadratic

A bandpass filter with central frequency ω_0 and -3-dB bandwidth ω_c (all frequencies are in rad/s) can be designed using a so-called *low-pass equivalent* filter with bandwidth ω_c. If we denote the Laplace operator for the low-pass case by s' and the Laplace operator for the bandpass case by s, the following frequency transformation can be used:

$$s'=s+\frac{\omega_0^2}{s}. \quad (66)$$

By this transformation the order of the filter doubles. If this transformation is applied to an integrator with transfer function $1/s$, a biquad with transfer function

$$b(s)=\frac{1}{s'}=\frac{s}{s^2+\omega_0^2} \quad (67)$$

results. This means that we can construct a bandpass filter by replacing every integrator in an appropriate low-pass filter by an appropriate biquad. The bandwidth and the filter characteristics (passband and stopband shape) of the resulting filter are determined by the properties of the low-pass equivalent filter, while its central frequency will be determined by the biquads.

The quality factor of the resulting bandpass filter can be computed as follows:

$$Q=\frac{\omega_0}{\omega_c}. \quad (68)$$

8.2. Linear

The low-pass equivalent filter, introduced in the previous section can, in turn, be derived from a *normalized low-pass equivalent* filter. This normalized filter has unity bandwidth and the non-normalized low-pass equivalent filter can be derived from it using the frequency transformation:

$$s''=\frac{s'}{\omega_c}. \quad (69)$$

s'' is the Laplace variable describing the normalized case.

Some properties of these normalized filters related to the corresponding non-normalized filters must be established. If $\boldsymbol{A}'$, $\boldsymbol{B}'$, $\boldsymbol{C}'$, $\boldsymbol{D}'$, $\boldsymbol{W}'$, and $\boldsymbol{K}'$ refer to the non-normalized filter, and $\boldsymbol{A}''$, $\boldsymbol{B}''$, $\boldsymbol{C}''$, $\boldsymbol{D}''$, $\boldsymbol{W}''$, and $\boldsymbol{K}''$ to the normalized filter, one can easily prove the following.

$$\boldsymbol{A}''=\frac{\boldsymbol{A}'}{\omega_c} \quad (70)$$

$$\boldsymbol{B}''=\frac{\boldsymbol{B}'}{\omega_c} \quad (71)$$

$$\boldsymbol{C}''=\boldsymbol{C}' \quad (72)$$

$$\boldsymbol{D}''=\boldsymbol{D}' \quad (73)$$

$$\boldsymbol{W}''=\omega_c\boldsymbol{W}' \quad (74)$$

$$\boldsymbol{K}''=\frac{1}{\omega_c}\boldsymbol{K}'. \quad (75)$$

If a bandpass filter is designed using the two transformations described here, the dynamic range properties of the final filter can be stated in terms of the properties of the normalized low-pass equivalent filter and the transformations.

IX. Dynamic Range Optimization

9.1. General

To optimize the dynamic range of a scaled filter we will turn to expression (27) to see how it can be maximized. There is one method to optimize this expression known.

More — on the outside.

This method has been published by Mullis and Roberts [10] and assumes that all the internal noise spectra are equal. As we will see for high-Q bandpass filter this assumption can be made. We thus state that $S_{n,i} = S_n$ for any i. We now rewrite (27) as

$$DR = \frac{U_{max}^2 \frac{1}{2\pi}\int_{-\infty}^{\infty} |H(j\omega)|^2 \, d\omega}{S_n \sum_{i=1}^{n} k_{ii} w_{ii}}. \tag{76}$$

H and U_{max} are independent of the filter network. Also, S_n is assumed to be known. In this case the dynamic range is maximal if $\Sigma_{i=1}^{n} k_{ii} w_{ii}$ is minimal. Mullis and Roberts have proved that $\Sigma_{i=1}^{n} k_{ii} w_{ii}$ is minimal if the following two restrictions are met:

$$\boldsymbol{D}_0^{-1} \boldsymbol{K} \boldsymbol{D}_0^{-1} = \boldsymbol{D}_0 \boldsymbol{W} \boldsymbol{D}_0 \tag{77}$$

$$k_{ii} w_{ii} = k_{jj} w_{jj} \tag{78}$$

for some diagonal matrix $\boldsymbol{D}_0$ and any i, j satisfying $1 \leqslant i, j \leqslant n$. In that case $\Sigma_{i=1}^{n} k_{ii} w_{ii}$ reaches its minimum value of

$$\left(\sum_{i=1}^{n} k_{ii} w_{ii} \right)_{min} = \frac{1}{n} \left(\sum_{i=1}^{n} \mu_i \right)^2 \tag{79}$$

where μ_i^2, $1 \leqslant i \leqslant n$ are the eigenvalues of the matrix $\boldsymbol{KW}$, which are independent of the realization. The minimum, reflected by (79) is therefore only dependent on the transfer function of the filter. A method to design a filter that reaches this optimum is also known [10]. We will not discuss this method here, because the filters that are obtained in this way are too difficult to realize. In an example to follow we will see that some of the more conventional filter architectures come close enough to this optimum.

In our filtering context the numbers μ_i are called the *second-order modes* of the transfer function. If we want to know what the optimal dynamic range of a filter is we must determine these values. On a computer the second-order modes can be determined as the square roots of the eigenvalues of the product $\boldsymbol{KW}$ of some realization. For calculations by hand this cannot be deemed practical. We can, however, give a lower limit for the sum of the second-order modes directly from the transfer function:

$$\sum_{i=1}^{n} \mu_i \geqslant \frac{1}{2} H(0). \tag{80}$$

(The proof is omitted.) We can now formulate the following theorem.

Theorem 1: If the dynamic range of a filter is properly described by (76) (which implies equal noise spectra) the dynamic range is never larger than the following value:

$$DR_{opt} \leqslant \frac{U_{max}^2}{S_n} \cdot \frac{4n \frac{1}{2\pi}\int_{-\infty}^{\infty} |H(j\omega)|^2 \, d\omega}{|H(0)|^2}. \tag{81}$$

This theorem relates the maximal dynamic range of a filter to its noise bandwidth. This theorem is an invaluable help to estimate the maximal dynamic range that can be attained with a filter in a simple way directly from the transfer function.

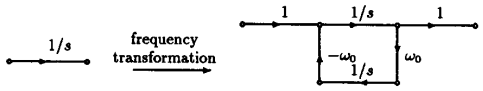

Fig. 5. If a frequency transformation is performed on a filter, every integrator in the filter is replaced by a biquad. Here a suitable example of such a biquad is shown.

9.2. *Frequency Transformed Filters*

9.2.1. Biquadratic: As pointed out in Section VIII, frequency transformation implies the substitution of a biquad for every integrator in the original filter. This multiplies the order of the filter by two. In order to make the distinction clear, when talking about low-pass to bandpass transformation we will designate the order of the low-pass equivalent filter by n and the order of the bandpass filter by N, so

$$N = 2n. \tag{82}$$

The biquad must have a suitable transfer function H (dictated by (67)) and preferably must meet the optimality criteria (64) and (65). A suitable biquad is depicted in Fig. 5. We see that if a filter is constructed in this way, every integrator comprising this filter will have one branch a_{ij} for which $|a_{ij}| = \omega_0$ connected to its input. All other branches (if any) connected to the same input will stem from the original filter. This filter is assumed to have a bandwidth ω_c that is much smaller than ω_0, because we are dealing with high-Q filters. If the original filter is designed neatly, all the branches of the original filter have values of the same order of magnitude as ω_c and have corresponding noise spectra. Now by (15) the noise production of the integrators of the transformed filter are dominated by the branch having absolute value ω_0. Therefore,

$$S_{n,i} = S_n = \frac{2kT\xi\omega_0 N}{C}. \tag{83}$$

The capacitors C_i are chosen equal to a common value C/N here, to make all noise spectra equal.

For these biquads we can easily prove that (58) and (59) are no longer approximations but exact. Also, comparing (67) and (44) we obtain the relations (84):

$$\begin{aligned} c_1 b_1 + c_2 b_2 &= 1 \\ c_1 b_2 - c_2 b_1 &= 0. \end{aligned} \tag{84}$$

This property will be used to derive the properties of frequency transformed filters.

The change of order in the transformation makes it necessary to renumber the states. State i in the original filter will be represented by states $2i-1$ and $2i$ (contained in biquad i) in the "image" filter.

With $s = j\omega$, $s' = j\omega'$ and (66) one gets

$$\frac{1}{2\pi}\int_{-\infty}^{\infty}|H(j\omega)|^2\,d\omega = \frac{1}{2\pi}\int_{-\infty}^{\infty}|H'(j\omega')|^2\,d\omega'. \quad (85)$$

This means that in order to evaluate the integral of the squared magnitude of the transfer function of the bandpass filter, one can evaluate the same integral for the corresponding (non-normalized) low-pass equivalent filter.

The gramians of the original filter are denoted by $\boldsymbol{K}'$ and $\boldsymbol{W}'$ and the gramians of the image filter by $\boldsymbol{K}$ and $\boldsymbol{W}$. So suppose that we have the controllability gramian of the original filter:

$$\boldsymbol{K}' = \begin{pmatrix} k'_{11} & k'_{12} & \cdots & k'_{1n} \\ k'_{21} & k'_{22} & \cdots & k'_{2n} \\ \vdots & \vdots & \ddots & \vdots \\ k'_{n1} & k'_{n2} & \cdots & k'_{nn} \end{pmatrix}$$

then one can prove that the controllability gramian of the image filter is

$$\boldsymbol{K} = (b_1^2 + b_2^2)\begin{pmatrix} k'_{11} & 0 & k'_{12} & 0 & \cdots & k'_{1n} & 0 \\ 0 & k'_{11} & 0 & k'_{12} & \cdots & 0 & k'_{1n} \\ k'_{21} & 0 & k'_{22} & 0 & \cdots & k'_{2n} & 0 \\ 0 & k'_{21} & 0 & k'_{22} & \cdots & 0 & k'_{2n} \\ \vdots & \vdots & \vdots & \vdots & \ddots & \vdots & \vdots \\ k'_{n1} & 0 & k'_{n2} & 0 & \cdots & k'_{nn} & 0 \\ 0 & k'_{n1} & 0 & k'_{n2} & \cdots & 0 & k'_{nn} \end{pmatrix}. \quad (86)$$

Similarly:

$$\boldsymbol{W} = (c_1^2 + c_2^2)\begin{pmatrix} w'_{11} & 0 & w'_{12} & 0 & \cdots & w'_{1n} & 0 \\ 0 & w'_{11} & 0 & w'_{12} & \cdots & 0 & w'_{1n} \\ w'_{21} & 0 & w'_{22} & 0 & \cdots & w'_{2n} & 0 \\ 0 & w'_{21} & 0 & w'_{22} & \cdots & 0 & w'_{2n} \\ \vdots & \vdots & \vdots & \vdots & \ddots & \vdots & \vdots \\ w'_{n1} & 0 & w'_{n2} & 0 & \cdots & w'_{nn} & 0 \\ 0 & w'_{n1} & 0 & w'_{n2} & \cdots & 0 & w'_{nn} \end{pmatrix}. \quad (87)$$

Here, b_1, b_2, c_1, and c_2 refer to the biquad. The proof of these relations is straightforward but long and tedious and does not contribute to understanding; therefore, it is omitted.

Suppose that $\boldsymbol{D}'_0 = \mathrm{diag}(d_1, d_2, \cdots, d_n)$ and

$$\boldsymbol{D}_0 = \sqrt[4]{\frac{b_1^2 + b_2^2}{c_1^2 + c_2^2}}\ \mathrm{diag}(d_1, d_1, d_2, d_2, \cdots, d_n, d_n).$$

Then it is clear that if (77) and (78) hold for the original filter,

$$\boldsymbol{D}_0'^{-1}\boldsymbol{K}'\boldsymbol{D}_0'^{-1} = \boldsymbol{D}'_0\boldsymbol{W}'\boldsymbol{D}'_0 \quad (88)$$

$$k'_{ii}w'_{ii} = k'_{jj}w'_{jj} \quad (89)$$

for $1 \leqslant i, j \leqslant n$, we also have for the image filter:

$$\boldsymbol{D}_0^{-1}\boldsymbol{K}\boldsymbol{D}_0^{-1} = \boldsymbol{D}_0\boldsymbol{W}\boldsymbol{D}_0 \quad (90)$$

$$k_{ii}w_{ii} = k_{jj}w_{jj} \quad (91)$$

for any $1 \leqslant i, j \leqslant 2n$. *This means that if the original filter is optimal the image filter will also be optimal.*

Note that this is also valid if the resulting filter is a low-Q filter. This also implies that the resulting bandpass filter is scaled if the original filter was scaled, which is also directly visible from (86).

9.2.2. Linear: Using (74) and (75) it is straightforward that a low-pass equivalent filter is optimal (in the sense that it obeys (77) and (78)) if and only if the corresponding normalized filter is optimal. If this result is combined with the results concerning biquadratic frequency transformation, the following theorem can be stated.

Theorem 2: If a bandpass filter is derived from a normalized low-pass equivalent filter, using (66) and (69), the derived filter is optimal in the sense that it obeys (77) and (78) if the normalized low-pass equivalent filter is optimal in the same sense and the biquads that are used satisfy optimality criteria (64) and (65).

This theorem shows how an optimal bandpass filter can be designed, starting from an optimal normalized low-pass equivalent filter. We will now determine the dynamic range properties of these optimal frequency transformed filters.

9.3. Dynamic Range of Optimal Transformed Filters

Using the gramians of the image filter, as computed in the previous subsection we will determine the dynamic range of the image filter. An important thing to notice first is derived from (84):

$$(b_1^2 + b_2^2)(c_1^2 + c_2^2) = (b_1c_1 + b_2c_2)^2 + (b_1c_2 - b_2c_1)^2 = 1. \quad (92)$$

Here, b_i and c_i refer to the structure of the biquads used to replace the integrators in the transformation.

From (82), (86), (87), and (92), we see:

$$\sum_{i=1}^{\bar{N}} k_{ii}w_{ii} = 2\sum_{i=1}^{n} k'_{ii}w'_{ii} \quad (93)$$

and from (74) and (75):

$$\sum_{i=1}^{n} k'_{ii}w'_{ii} = \sum_{i=1}^{n} k''_{ii}w''_{ii}. \quad (94)$$

The dynamic range of the image filter is given by (76). Equations (85) and (69) are then used to rewrite the dynamic range of the image filter as

$$DR = \frac{U_{\max}^2\omega_c}{S_n} \cdot \frac{\frac{1}{2\pi}\int_{-\infty}^{\infty}|H''(j\omega'')|^2\,d\omega''}{2\sum_{i=1}^{n} k''_{ii}w''_{ii}}. \quad (95)$$

The dynamic range of the bandpass filter is now ex-

More — on the outside.

pressed in terms of the properties of its low-pass equivalent. If this is combined with Theorem 2 the following is easy to see.

Theorem 3: If a bandpass filter is derived from a low-pass equivalent filter as described in Theorem 2, the bandpass filter is just as far from optimum as the corresponding normalized low-pass equivalent is, if it is assumed that the bandpass filter, as well as the low-pass equivalent, has equal internal noise sources that are independent of the network architecture, and the biquads that are used to substitute the integrators are optimal.

The assumption of equal internal noise sources is in general not true for low-pass filters, but it is true for high-Q bandpass filters if they are designed as outlined in this paper (see (83)). This makes the notion of low-pass filters with equal internal noise spectra valuable if those low-pass filters are used as low-pass equivalents of bandpass filters to be designed.

With (83), (95) can be written as

$$DR = \frac{U_{\max}^2 C}{4kT\xi NQ} \cdot \frac{\frac{1}{2\pi}\int_{-\infty}^{\infty} |H''(j\omega'')|^2 \, d\omega''}{\sum_{i=1}^{n} k_{ii}'' w_{ii}''}. \quad (96)$$

According to Theorem 2 the dynamic range of the bandpass filter is optimal if the dynamic range of the normalized low-pass equivalent is optimal, that is, if $\Sigma_{i=1}^{n} k_{ii}'' w_{ii}''$ is minimal. Due to (79) this minimum is $n^{-1}(\Sigma_{i=1}^{n} \mu_i'')^2$. Here, $\mu_i''^2$ represent the eigenvalues of the product $\boldsymbol{K}''\boldsymbol{W}''$. The optimal dynamic range for the bandpass filter is now

$$DR_{\text{opt}} = \frac{U_{\max}^2 \omega_c}{S_n} \cdot \frac{n\frac{1}{2\pi}\int_{-\infty}^{\infty} |H''(j\omega'')|^2 \, d\omega''}{2\left(\sum_{i=1}^{n} \mu_i''\right)^2}. \quad (97)$$

Now with (80) we can state the following theorem, which is a variant of Theorem 1.

Theorem 4: If a bandpass filter is designed by performing the transformations (66) and (69) on a normalized low-pass equivalent filter, an upper limit for its dynamic range is given by:

$$DR \leq \frac{U_{\max}^2}{S_n} \cdot \frac{N\frac{1}{2\pi}\int_{-\infty}^{\infty} |H(j\omega)|^2 \, d\omega}{|H(j\omega_0)|^2}. \quad (98)$$

In the same way as (95), this is rewritten as

$$DR_{\text{opt}} \leq \frac{U_{\max}^2 C}{2kT\xi Q} \cdot \frac{\frac{1}{2\pi}\int_{-\infty}^{\infty} |H''(j\omega'')|^2 \, d\omega''}{|H''(0)|^2}. \quad (99)$$

Remember that the normalized low-pass equivalent filter has (double-sided) −3-dB bandwidth 2, so that its noise bandwidth in most cases approximates the value $1/\pi$:

$$\frac{\frac{1}{2\pi}\int_{-\infty}^{\infty} |H''(j\omega'')|^2 \, d\omega''}{|H''(0)|^2} \approx \frac{1}{\pi}. \quad (100)$$

So now we have a very simple and crude approximation of the optimal dynamic range of a high-Q bandpass filter:

$$DR_{\text{opt}} \lesssim \frac{U_{\max}^2 C}{2\pi kT\xi Q}. \quad (101)$$

Now in expressions (96), (99), and (101), we have proved the important fact that the dynamic range of a high-Q bandpass filter is, even in the optimal case, inversely proportional to its quality factor. Also, the dependence on the total capacitance value is shown.

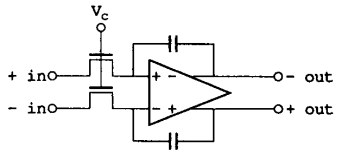

Fig. 6. A practical MOSFET-C integrator.

X. A Practical Design Example

After all this theory one can wonder if it really can be applied in a practical situation. Fortunately we can show that this is indeed the case and in this section we are therefore designing a real integratable filter. "Real" in this case means that we worked out the filter to the transistor level and made it work according to the circuit simulator SPICE. In this design it will become clear how we can benefit from the insights the theory in this paper offers us.

10.1. Design Procedure

We want to design an eighth-order Butterworth bandpass filter with a central frequency ω_0 of 2π(100 kHz) and a bandwidth ω_c of 2π(7 kHz), which implies $Q = 14.3$. This filter was initially designed as an IF-filter for AM radio [5] and is now redesigned in a different way to serve as an example in this context.

We want to realize a dynamic range of 70 dB. This is an arbitrary number which we use to show how one can design filters with a dynamic range demand that one states *in advance*.

We use as extrinsic integrator the structure depicted in Fig. 2(a). To make this structure tunable we replace the resistors by MOSFET's. To cancel second-order nonlinearities the structure is balanced. The structure we arrive at is depicted in Fig. 6. Only one (differential) input is shown.

The fact that on basis of this type of integrator one designs balanced filters causes, although of a minor type, some difficulties in the design procedure, for the designing is mainly done on one single-ended "half" of the

filter, while the results are to be calculated differentially. It is, however, easy to see that a single-ended filter with maximum integrator output signal level U_{max}^2 and total capacity C has the same dynamic range as a corresponding balanced filter with maximum *single-ended* integrator output level U_{max}^2 and total capacity C. The formulas we derived for the dynamic range therefore remain valid. For that reason we define for a differential filter U_{max}^2 as well as noise spectra single ended. The maximum output signal level of the filter $U_{max,out}^2$ and its noise output voltage $\overline{U_{n,o}^2}$ are defined differentially as those are the relevant output quantities. This may differ by a factor 2 or 4 in the formulas for the output noise and the maximum output signal level, but the formulas for the dynamic range remain unaltered.

If we have a supply voltage voltage V_{cc} of 5 V and a quiescent balance voltage V_{bal} of 2 V (this is the bias voltage at the inputs and outputs of the integrator) the control voltage V_c applied at the gates of the MOSFET's that represent the resistors should be no more than 4.5 V to retain enough tunability. In this case the maximum signal level U_{max} at the inputs of the integrators for at most 1% harmonic distortion is 0.7 V rms. As all the outputs of integrators are connected to inputs of other integrators and vice versa, this is also the maximum output voltage of the integrators.

By general theories concerning amplifier design, it is, in our context, in principle possible to design the opamp such that $\xi \approx 1$ [9]. It does not make sense to make ξ extremely close to 1, because that only costs supply power and does not enlarge the dynamic range appreciably once the noise factor is close to 1. Therefore, we initially assume that $\xi = 2$. With these data from (101) we see that to realize a dynamic range of 70 dB we at least need a total capacitance of 15 pF, which is quite acceptable. So this equation immediately gives us an idea of the feasibility of the filter.

As filter architecture we use the symmetrical ladder. The signal flow graph of the normalized low-pass equivalent filter is shown in Fig. 7. The order n of the low-pass equivalent is four while the order N of the bandpass filter is eight. The state matrices are

$$\boldsymbol{A}'' = \begin{pmatrix} -1.3065 & -0.7107 & 0 & 0 \\ 0.9950 & 0 & -0.4192 & 0 \\ 0 & 0.6987 & 0 & -0.4855 \\ 0 & 0 & 1.4564 & -1.3065 \end{pmatrix}$$

$$\boldsymbol{B}'' = \begin{pmatrix} 1.728 \\ 0 \\ 0 \\ 0 \end{pmatrix}$$

$$\boldsymbol{C}'' = (0 \quad 0 \quad 0 \quad 1)$$

$$\boldsymbol{D}'' = 0. \tag{102}$$

$\boldsymbol{W}$ and $\boldsymbol{K}$ are determined by numerically solving (10) and (11). The results:

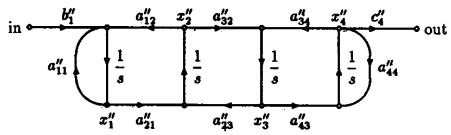

Fig. 7. The filter network: A symmetrical ladder.

$$\boldsymbol{W}'' = \begin{pmatrix} 0.3349 & 0.4397 & 0.1411 & -0.0524 \\ 0.4397 & 0.7175 & 0.4473 & -0.0688 \\ 0.1411 & 0.4473 & 0.7175 & 0.1287 \\ -0.0524 & -0.0688 & 0.1287 & 0.3349 \end{pmatrix} \tag{103}$$

$$\boldsymbol{K}'' = \begin{pmatrix} 1 & 0.2626 & -0.1404 & -0.1566 \\ 0.2626 & 1 & 0.6234 & 0.2878 \\ -0.1404 & 0.6234 & 1 & 0.8971 \\ -0.1566 & 0.2878 & 0.8971 & 1 \end{pmatrix}. \tag{104}$$

From (104) one can see that we already have scaled the filter. As the filter will continue to be scaled after transformation to a bandpass filter we do not have to worry about scaling anymore.

The dynamic range of the bandpass filter can already be determined using (96). By (28)

$$\frac{1}{2\pi}\int_{-\infty}^{\infty} |H''(j\omega'')|^2 \, d\omega'' = 1. \tag{105}$$

So by (96)

$$DR = 0.0594 \frac{U_{max}^2 C}{4kT\xi Q}. \tag{106}$$

The second-order modes are determined as the square roots of the eigenvalues of $\boldsymbol{KW}$: $\mu_1 = 0.02167$, $\mu_2 = 0.2264$, $\mu_3 = 0.8451$, $\mu_4 = 1.5151$. Therefore, by (97) and (83), the *optimal* dynamic range is

$$DR_{opt} = 0.0735 \frac{U_{max}^2 C}{4kT\xi Q}. \tag{107}$$

Comparing these two teaches us that the scaled ladder filter is only 1 dB away from optimum, so the ladder filter is a nice choice in this situation.

From (106) with $U_{max} = .7$ V, $\xi = 2$, and $Q = 100/7$, we now can say that in order to realize a dynamic range of 70 dB we need a total capacitance of 163 pF, which is 20 pF per integrator, or 10 pF per capacitor since each integrator contains two capacitors. So we put $C_i = 10$ pF for $i = 1, \cdots, 8$, so that $\Sigma_{i=1}^{8} C_i = (1/2)C$.

Now the filter is denormalized. The state matrices of the denormalized low-pass equivalent filter are given by (70) to (72). A bandpass filter is realized by substituting in this filter a biquad for each integrator. The signal flow diagram of the biquad we use is shown in Fig. 5. Fig. 8 shows a realization of such a biquad. Here, MOSFET's are used as resistors. These resistors should have a value of $1/C_i\omega_o = 159$ kΩ as explained in Section IV. With the values and parameters we have (i.e., $V_{bal} = 2$ V, $V_c = 4.5$ V, the transconductance parameter $\beta_\square = 45$ μA/V,

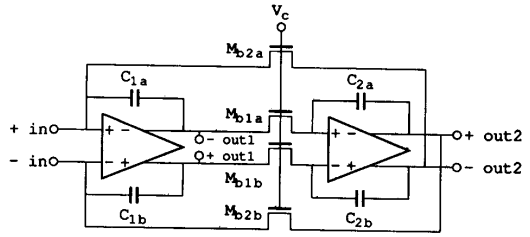

Fig. 8. A realization of a biquad that can be used as a building block for a bandpass filter. The capacitors are 10 pF each, and the MOSFET's have a length of 21 μm and a width of 3 μm. In order to compensate for the parasitic poles in the opamps resistors of 5300 Ω had to be connected in series with C_{2a} and C_{2b}.

threshold voltage including body effect $V_{TB} = 1.5$ V),[1] the MOSFET should have a width of 3 μm and a length of 21 μm. Initial simulations on this circuit showed the need to connect extra damping resistors of 5300 Ω in series with C_{2a} and C_{2b} to compensate parasitic poles caused by the opamps. For a really accurate design these resistors should be made controllable so that (apart from the mentioned ω_0-tuning loop) an independent automatic Q-tuning loop can be added to the circuit, as indicated by Chiou *et al.* [11] and Vanpeteghem *et al.* [12].

The connections between the biquads should also be realized with MOSFET's that are used as resistors. Then each pair of resistors represents one entry of the matrix $\boldsymbol{A}'$ or $\boldsymbol{B}'$: $R_{aij} = 1/(C_i|a'_{ij}|)$ and $R_{b1} = 1/(C_1|b'_1|)$. This looks straightforward enough, but if we try to realize this filter in this way we encounter one serious problem. The entries of $\boldsymbol{A}'$ and $\boldsymbol{B}'$ are much smaller than ω_0, so the corresponding resistors are much larger than the resistors in the biquad. To realize these resistors, very long and narrow MOSFET's are needed, giving rise to formidably dominant parasitic poles. One single simulation shows that for that reason the filter is not realizable in this way. This problem is a general problem in the realization of high-Q bandpass filters. It appears that we must look for another solution.

A very elegant solution is the coupling of the stages by capacitors instead of resistors. We can do that if we use the biquad outputs numbered 2 instead of outputs 1 in Fig. 8. The filter then is realized as depicted in Fig. 9. The capacitors are determined as $C_{aij} = C_i|a'_{ij}/\omega_0|$ or $C_{b1} = C_1|b_1/\omega_0|$; they are small compared to the capacitors in the biquad so that the total capacitance used is not enlarged severely.

The opamp we use originates from Banu *et al.* [13]. It is depicted in Fig. 10. It has an internally balanced output with an adjustable balance level. A SPICE simulation of one such an opamp shows that it has a noise factor ξ of 1.32 in our context. This finally enables us to calculate the dynamic range of this filter using (106):

$$DR = 71.7 \text{ dB}. \tag{108}$$

[1]The transistor parameters refer to the Philips Bimos Process we use.

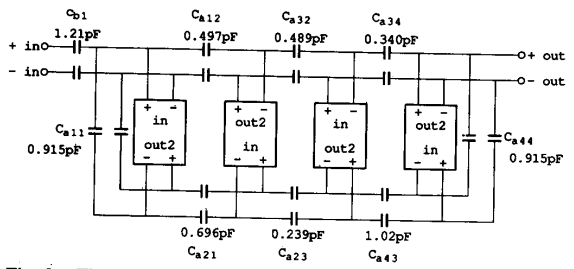

Fig. 9. The connection of the biquads with capacitors. $C_{aij} = C_i|a'_{ij}/\omega_0|$.

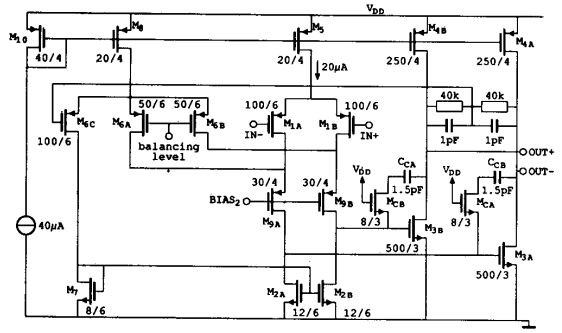

Fig. 10. A suitable balanced opamp.

This is what we wanted to achieve. To get a better grasp on the operation of the filter we can also calculate the noise output and the maximum output signal. This is done by rewriting the equations for these (i.e., (20) and (24) with (25)) in terms of the properties of the normalized low-pass equivalent filter, that is, in $\boldsymbol{W}''$ and $\boldsymbol{K}''$. The differential mode noise output $\overline{U_{n,o}^2}$ is two times the single ended noise output. The single ended noise output is calculated with $(1/2)C$ as total capacitance. We thus obtain by (20), (74), (83), and (87):

$$\overline{U_{n,o}^2} = 2\sum_{i=1}^{N} S_{n,i} w_{ii}$$

$$= 2\frac{2kT\xi\omega_0 N}{\frac{1}{2}C}\sum_{i=1}^{N} w_{ii}$$

$$= 2\frac{2kT\xi\omega_0 N}{\frac{1}{2}C}\cdot\frac{2\sum_{i=1}^{n} w''_{ii}}{\omega_c} = (3.63\cdot 10^{-4}\text{ V})^2. \tag{109}$$

The maximum differential mode output signal level $\overline{U_{max,out}^2}$ is four times the single ended maximum signal level, not two times as in the noise case because here the signals in the two paths are correlated. We had defined U_{max} single-ended, so the maximal differential output

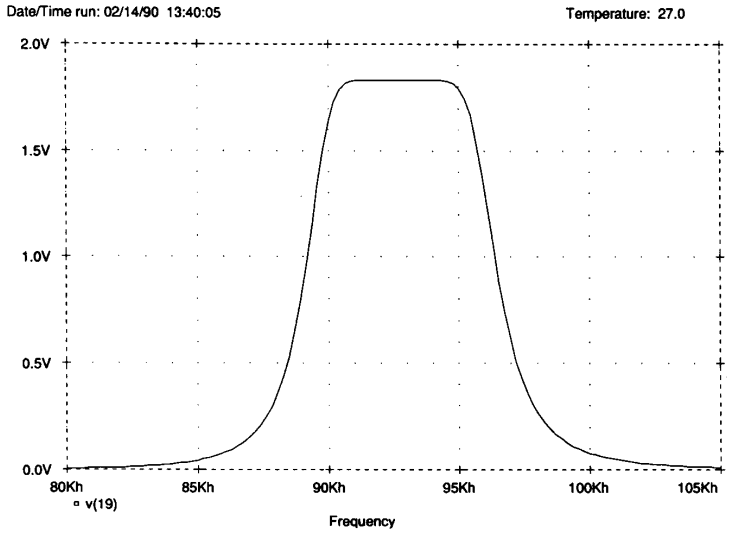

Fig. 11. The magnitude of the transfer function of the filter as calculated by SPICE.

signal level is, by (24) and (25),

$$\overline{U_{\max,\text{out}}^2} = 4\frac{U_{\max}^2\frac{1}{2\pi}\int_{-\infty}^{\infty}|H(j\omega)|^2\,d\omega}{\max_i k_{ii}}$$

$$= 4\frac{U_{\max}^2\omega_c\frac{1}{2\pi}\int_{-\infty}^{\infty}|H''(j\omega'')|^2\,d\omega''}{\omega_c\max_i k''_{ii}}$$

$$= 4U_{\max}^2 = (1.4\text{ V})^2. \tag{110}$$

We used (85), (69), (75), and (86) to do this derivation.

10.2. Results from Simulation

Now the filter is fully designed up to the transistor level. To validate our design we have simulated it with SPICE. The results are discussed below.

The transfer function is shown in Fig. 11. The central frequency is a little lower than 100 kHz, but that is a matter of tuning. The shape of the transfer function is accurately what was designed for. The noise output spectrum is shown in Fig. 12.[2] This noise spectrum was integrated numerically (over a wider range than shown in the figure), to yield a total output noise voltage of $3.67\cdot 10^{-4}$ V. Note how well this fits with our theoretical outcome in (109).

Fig. 13 shows the f_i (the transfers from the input of the filter to the outputs of the biquads) of the filter. If these functions are integrated as indicted by (17) and (19) the diagonal entries of $\boldsymbol{K}$ can be determined from the simulation.[3] This we also have done numerically with the following results.

$$k_{11} = k_{22} = 4.50\cdot 10^4\text{ rad/s} \tag{111}$$

$$k_{33} = k_{44} = 4.38\cdot 10^4\text{ rad/s} \tag{112}$$

$$k_{55} = k_{66} = 4.44\cdot 10^4\text{ rad/s} \tag{113}$$

$$k_{77} = k_{88} = 4.44\cdot 10^4\text{ rad/s}. \tag{114}$$

According to (75), (86), and (104), the diagonal entries of $\boldsymbol{K}$ should have the value $\omega_c = 4.40\cdot 10^4$ rad/s, so that this also fits well with theory. We also can see that

$$\frac{1}{2\pi}\int_{-\infty}^{\infty}|H(j\omega)|^2\,d\omega = k_{88} = 4.44\cdot 10^4\text{ rad/s}. \tag{115}$$

Now at last we can determine the dynamic range of the filter from the results of the simulation. By (110):

$$\overline{U_{\max,\text{out}}^2} = 4\frac{U_{\max}^2\frac{1}{2\pi}\int_{-\infty}^{\infty}|H(j\omega)|^2\,d\omega}{\max_i k_{ii}} = (1.39\text{ V})^2. \tag{116}$$

The dynamic range is:

$$DR = \frac{\overline{U_{\max,\text{out}}^2}}{\overline{U_{\text{n,o}}^2}} = 71.6\text{ dB}. \tag{117}$$

This fits quite well with our theoretical outcome in (108).

[2]SPICE lacks a correct noise model for MOSFET's biased in the triode region. Therefore, the MOS resistors were replaced by ordinary resistors for this particular simulation. This accounts for the fact that from Fig. 12 a slightly different central frequency is observed than from the other figures.

[3]As the spectra are to be integrated double sided (i.e., also for negative frequencies) the values obtained are to be multiplied by 2. This is not to be done to the noise spectrum, for SPICE calculates noise spectra single sided.

More — on the outside.

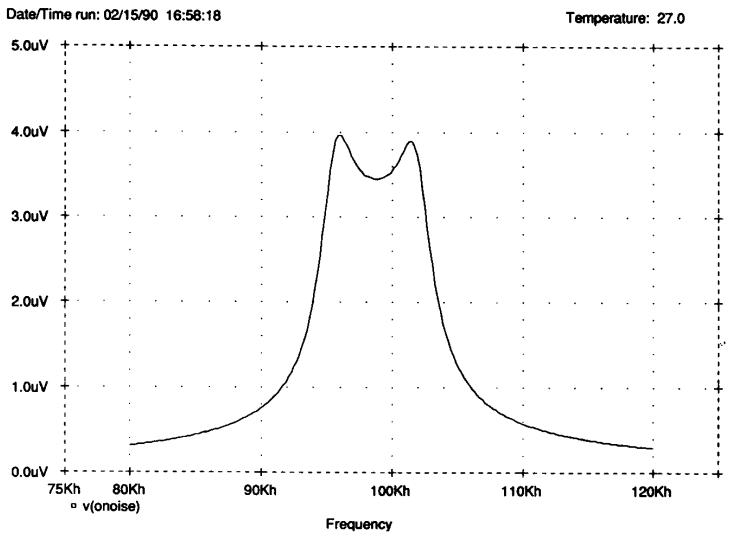

Fig. 12. The output noise spectrum of the filter, by SPICE. Along the ordinate the square root of the noise output spectrum ($\sqrt{S_{n,out}}$) is plotted.

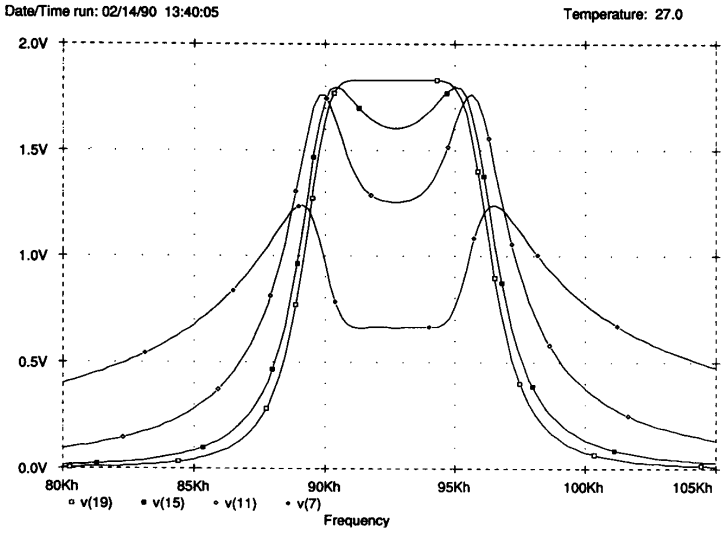

Fig. 13. The internal transfer functions f_i of the filter for $i \in \{2,4,6,8\}$. The corresponding transfers for $i \in \{1,3,5,7\}$ are identical.

XI. Conclusions

We have established a method to design high-Q bandpass filters with a prescribed dynamic range. From the theory we have developed it is clear what the fundamental restrictions for the dynamic range of such a filter are. Knowing these restrictions and the technology used one can say beforehand if a filter one wants to design is feasible. The usefulness of the theories is shown by the design of a complete bandpass filter, up to the transistor level, of which it was shown by simulations that it indeed featured the prescribed dynamic range, not excessively more, but certainly not less.

The methods offer prospects of automatically designing (semi-) optimal filters.

References

[1] K. W. Moulding, J. R. Quartly, P. J. Rankin, R. S. Thompson, and G. A. Wilson, "Gyrator video filter IC with automatic tuning," *IEEE J. Solid State Circuits*, vol. SC-15, pp. 963–968, Dec. 1980.

[2] J. O. Voorman, W. H. A. Brüls, and P. J. Barth, "Integration of analog filters in a bipolar process," *IEEE J. Solid-State Circuits*, vol. SC-17, pp. 713–722, Aug. 1982.

[3] B. Song and P. R. Gray, "Switched-capacitor high-Q bandpass filters for IF applications," *IEEE J. Solid-State Circuits*, vol. SC-21, pp. 924–933, Dec. 1986.

[4] Y. Tsividis, M. Banu, and J. Khoury, "Continuous-time MOSFET-C

More — on the outside.

filters in VLSI," *IEEE Trans. Circuits Systems*, vol. CAS-33, Feb. 1986.
[5] G. Groenewold, "Integrated selectivity for AM-receives," in *Proc. Conf. ESSCIRC*, pp. 354–357, 1988.
[6] B. Nauta and E. Seevinck, "A 110 MHz CMOS transconductance-C low-pass filter," in *Proc. Conf. ESSCIRC*, pp. 141–144, 1989.
[7] G. Espinosa, F. Montecchi, E. Sánchez-Sinencio, and F. Maloberti, "Noise performances of ota-c filters," in *Proc. IEEE ISCAS*, vol. 3, pp. 2173–2176, 1988.
[8] G. Groenewold, "The design of high dynamic range analog continuous-time integratable filters," Internal Rep., Delft Univ. Technology, Dept. Electr. Eng., 1990.
[9] E. H. Nordholt, *Design of High-Performance Negative Feedback Amplifiers*. Amsterdam: Elsevier, 1983.
[10] C. T. Mullis and R. A. Roberts, "Synthesis of minimum roundoff noise fixed point digital filters," *IEEE Trans. Circuits Syst.*, vol. CAS-23, pp. 551–562, Sept. 1976.
[11] C.-F. Chiou and R. Schaumann, "Design and performance of a fully integrated bipolar 10.7-MHz analog bandpass filter," *IEEE Trans. Circuits Syst.*, vol. CAS-33, pp. 116–124, Feb. 1986.
[12] P. M. Vanpeteghem and R. Song, "Tuning strategies in high-frequency integrated continuous-time filters," *IEEE Trans. Circuits Syst.*, vol. 36, pp. 136–139, Jan. 1989.
[13] M. Banu, J. M. Khoury, and Y. Tsividis, "Fully differential operational amplifiers with accurate output balancing," *IEEE J. Solid-State Circuits*, vol. 23, pp. 1410–1414, Dec. 1988.

Gert Groenewold received the M.S. degree in electrical engineering from the Delft University of Technology in The Netherlands in 1988.

Subsequently he joined the Electronics Laboratory at Delft to work towards a Ph.D. thesis. His research includes developing a formal design theory for analog integrated filters along with the development of software.

More — on the outside.